Drained-undrained response and other fundamental aspects of granular materials using DEM

Mauricio Pinheiro, Richard G. Wan
Dept. of Civil Engineering, University of Calgary, Calgary, Alberta, Canada
Qiang Li
Golder Associates, Calgary, Alberta, Canada

ABSTRACT
In this paper we have chosen the discrete element method to investigate the effects of initial confining pressure and initial density on the granular material behaviour under both drained and undrained conditions. The influence of micromechanical parameters and particle rotations on the shear strength and dilatancy characteristics of the granular assembly is also examined. Finally we have established a correlation between the evolution of some micro-variables and macro-phenomena. We did not quantitatively compare our numerical results to any laboratory test on real soil; rather we outlined some capabilities of the discrete approach to qualitatively emulate granular material. We conclude that this approach is an efficient and robust tool to explore the constitutive behaviour of granular materials.

RÉSUMÉ
Dans cet article nous recherchons les effets de la pression de confinement et la densité initiale sur le comportement d'un matériau granulaire sous des conditions drainées et non-drainées par la méthode des éléments discrets. Nous étudions notamment l'influence des paramètres micromécaniques ainsi que la rotation de particules sur la résistance au cisaillement et la dilatance du matériau. Entre autres, on a établit la corrélation entre l'évolution de quelques paramètres micromécaniques et des phénomènes macroscopiques. Aucune tentative n'a été faite pour comparer les résultats numériques avec le comportement réel des sols car le but principal est de démontrer les capacités d'un modèle discret de décrire assez fidèlement le comportement d'un matériau granulaire. Nous concluons que cette approche discrète s'avère être très utile pour étudier le comportement micromécanique des matériaux granulaires.

1 INTRODUCTION

The study of granular materials with a focus to their discrete nature requires the selection of a suitable numerical method for their modeling. Accordingly, the three-dimensional particle flow code PFC3D (Itasca, 1999) was chosen as a research tool to conduct all the simulations reported in this paper. This tool allowed us to gain invaluable insights in the micromechanical characteristics that lead to salient features of the global behaviour of granular materials. Here a brief introduction to discrete element method is first given. In the following part, the discrete element model is calibrated and the effects of some micro parameters, such as interparticle friction and particle rotation on the constitutive behaviour of granular materials are also discussed. Typical stress-strain behaviours of sands are next presented for both monotonic conventional triaxial drained and undrained compression tests. The effects of the initial void ratio and confining pressure on both drained and undrained behaviours are examined. Furthermore, micro level variables such as both the coordination number and fabric evolutions during the drained shear process are also provided at the end of this paper.

2 OVERVIEW ON DEM

The discrete element method (DEM) is a numerical tool that models the movement and interaction of individual of particles within a system subjected to external loads. It was first introduced for the analysis of rock mechanics problems (Cundall, 1971), and then applied to granular materials as described by Cundall and Strack (1979). Engineering problems, such as the flow of granular materials which exhibit very large-scale discontinuous dynamic behaviour, may not be properly solved within a continuum approach such as the finite element method. DEM has provided a numerical means for analyzing the progressive movements and interactions of bodies in granular assemblies with Newton's second law being applied to each particle within the system. The continual movement of each particle results from the non-equilibrium of various forces exerted on it. DEM explicitly models the dynamic motion and mechanical interaction of each particle at discrete points in time, with each point being termed as a step. For this purpose, the integration of equations of motion and contact laws, as well as the detection of contacts, is necessary. The latter is the core of each DEM code and is the most time consuming part.

The main advantage of the discrete element method is its simplicity compared to most of the constitutive models, which normally employ a large amount of parameters; some of them often have no physical meaning. By using DEM, the need for complex constitutive models is avoided, besides other computational difficulties related to some particular features of the mechanical behaviour of granular soils (strain softening, strain localization and non-associative flow rule). On the other hand, a key limitation of DEM is that associated with modeling large number of particles within a soil volume. Despite that limitation, the discrete element approach offers an important and useful tool to develop our understanding of the fundamental mechanisms that determine soil response. Computer simulations are expected to bring a better understanding of qualitative phenomena like arching effects, stress-dilatancy, and strain localization. By recognizing that both phenomenological and discrete element approaches have merits and limitations, the discrete and continuum mechanics should be viewed as complementary, but not adversary tools to model the constitutive behaviour of granular materials.

3 MODEL DESCRIPTION

The DEM model used in this study is intended to be small, but yet statistically equivalent to a volume of real sand. Initially, spheres are generated randomly in a cubic box so as to achieve a uniform particle size distribution for a given void ratio. The resulting 3D assembly consists of about 2000 rigid and weightless spherical particles of different sizes, randomly assembled to form a cubic specimen with a side length of 31.4 mm. The initial void ratios achieved at a confining pressure of 100 kPa were 0.658 and 0.779 for the dense and loose samples, respectively. The number of particles may vary slightly with the initial void ratio. The radius of the spherical particles in the assembly ranges from 1.0 to 1.6 mm. Each particle and contact has prescribed properties such as density, normal and tangential contact stiffness, and inter-particle friction coefficient, as listed in Table 1. The basic friction angle is fixed to a value representative for granular materials, that is φ_μ = 26.5º, so the inter-particle friction coefficient is $\mu = \tan \varphi_\mu = 0.5$. The density of particles was set to a typical value for quartz sand. The defaulted local non-viscous damping coefficient is used to achieve the equilibrium state in the numerical simulations. These parameters are chosen to ensure that sphere (or contact) overlaps during the program execution are small and that the numerical results are stable and accurate.

Table 1. Micro-properties for the discrete assembly

Micro-properties	Values
Minimum radius, R_{min} (mm)	1.0
Radius ratio, R_{max}/R_{min}	1.6
Particle density, ρ_p (kg/m^3)	2650.0
Particle contact modulus, E_c (MPa)	88.0
Particle normal/shear stiffness, k_n/k_s	1.0
Particle friction coefficient, μ	0.5

3.1 Influence of interparticle friction coefficient

The interparticle friction angle is an intrinsic parameter required by PFC3D. It differs from the bulk friction angle in that it relates to the friction generated between the particle surfaces when one particle slides slowly over another. In physical experiments, it is somewhat difficult to change the interparticle friction, for the value of friction coefficient is usually constant for certain materials. By contrast, this is not a problem in the case of numerical simulations as the interparticle friction coefficient can be simply changed.

Here, the dense specimen case is selected to examine the effects of interparticle friction on shear strength and stress-dilatancy of granular materials. Figure 1 shows the deviatoric over mean stress ratio (q/p) [$q = \sigma_1 - \sigma_3$; $p = 1/3\cdot(\sigma_1 + 2\sigma_3)$] versus the axial strain and the volumetric strain versus axial strain curves for sand samples with different interparticle friction coefficients spanning from 0.0 to 100. Here the upper limit of 100 is simply used for illustrative purposes. When the friction coefficient is below 0.5, the stress ratio curves increase monotonically. There is an obvious peak in the stress ratio plot when the interparticle friction reaches 0.5, and the peak becomes more pronounced when the friction coefficient reaches 100. The trend is that the peak stress ratio increases with the increase in the interparticle friction coefficient. Even for the case of null friction coefficient the sample shows a tendency to dilate, and the dilation rate increases with the increase of the friction coefficient. In all simulations, an initial confining pressure of 100 kPa was applied.

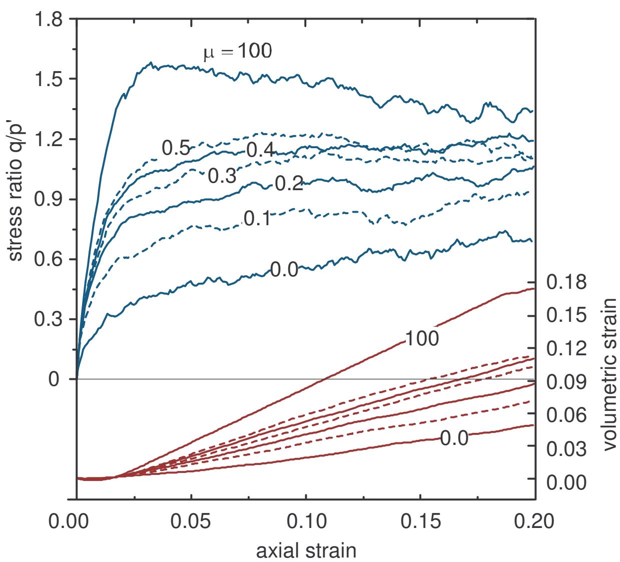

Figure 1. Effects of interparticle friction on shear strength and dilatancy characteristics of DEM model

3.2 Influence of stiffness ratio

The normal (k_n) and tangential (k_s) contact stiffnesses between particles appear to be an arbitrary parameter and as such it is important to investigate their impact on the global response of an assembly of particles. The elastic parameters (Young's modulus and Poisson's ratio) surely are function of the interparticle contact stiffnesses as well as the particle packing, as can be demonstrated by a micromechanical analysis (see Chang et al. 1992). In this section, we investigate the effect of the stiffness ratio k_n/k_s on the stress and volumetric responses using the dense particle assembly.

The stress ratio versus axial strain curves are shown in Figure 2 for several different stiffness ratios. From this figure, we can see some slight differences between the curves. If we zoom in at the origin (see inset), we notice that the slope, and therefore, the Poisson's ratio, increases as the stiffness ratio increases. Again, an initial confining pressure of 100 kPa was applied in all the simulations carried out.

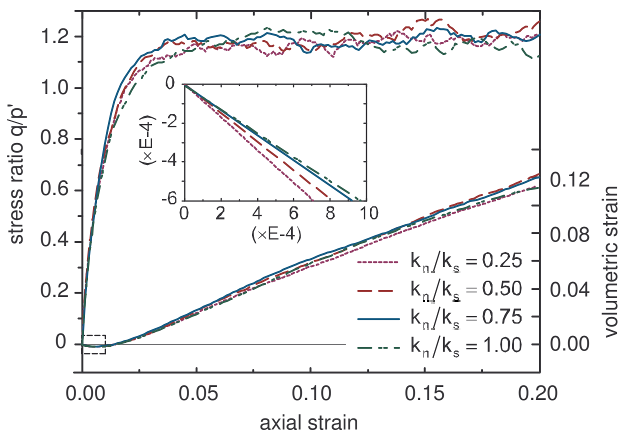

Figure 2. Effects of stiffness ratio on shear strength and dilatancy characteristics of DEM model

3.3 Influence of particle rotation

Particle rotation is known to have an important influence on the constitutive behaviour of granular materials, particularly for circular or spherical particles (Bardet, 1994). The role of particle rotation was verified in the experiments performed by Oda et al. (1982) using photoelastic disks. He showed that the peak strength is almost independent of the interparticle friction, which is unusual, and attributed this to the dominant role of inter-particle rolling as a microscale mechanism in granular materials. In this section, we implemented a short code in FISH (a programming language embedded in PFC that enables user to define new variables and functions) to prevent the rotation of particles during the shear process. The particle assembly used here is exactly the same as the ones for dense and loose specimens in the previous simulations except for the rotation prohibition. As shown in Figure 3, the stress ratio for both specimens increases sharply up to 2.0, which corresponds to the mobilized friction angle of 49º. This value is too high for real sand. For the loose specimen, dilation starts taking place at 4 % axial strain, which is earlier than the case with free particle rotation. For both dense and loose samples, the dilation rate is larger than the case with free particle rotation.

From these plots, it is concluded that particle rotation plays an important role in the dilatancy characteristics of sands. The restriction of particle rotations could contribute to the increase in the strength as well as the dilation rate of the granular assembly.

4 MONOTONIC DRAINED LOADING

The following discussions demonstrate the capability of the discrete element model to capture pressure and initial void ratio dependencies in a consistent manner under the drained conditions. Various initial void ratios and confining pressures are used in this numerical exercise.

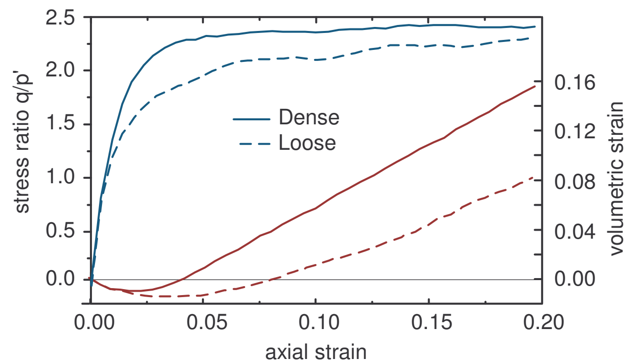

Figure 3. Effects of particle rotation on shear strength and dilatancy characteristics of DEM model

4.1 Influence of initial void ratio

Density dependency is one of the most important features of granular materials since different initial void ratios (or density states: dense, medium, and loose) lead to distinct stress-strain responses under both drained and undrained conditions (Mitchell and Soga, 2005). In our simulations, dense, medium-dense, and loose samples were created by assigning a predefined contact friction coefficient of 0.5 to all particles contained within an assembly at initial void ratios of 0.563, 0.786, and 0.887 respectively. A servo-control algorithm was then activated to compact the specimens and bring them into equilibrium under isotropic stress state of 100 kPa. The final void ratios reached after consolidation were 0.651, 0.770, and 0.808 for the dense, medium-dense and loose cases respectively. Once the desired stress state was reached for each density, the corresponding assembly configurations were saved for subsequent shear tests.

Starting from the initial isotropically compressed specimen, a set of numerical triaxial shear tests are carried out under drained condition. As such, both σ_2 and σ_3 are initially maintained at a constant confining pressure of 100 kPa, while the specimen is deformed at a constant strain rate in the direction coincident with the principal σ_1 stress direction. Such a strain controlled loading refers to conventional triaxial shearing tests in drained condition where the ratio $\Delta q/\Delta p$ is maintained at a value of three. In all numerical tests, the specimen is sheared until 20 % axial strain is reached.

Based on the void ratios used and the corresponding packing, the idealized granular material simulated here were meant to capture the behaviour of uniform rounded quartz sand like Ottawa sand. In the following part, the plots of stress ratio (q/p) and volumetric strain versus axial strain in drained compression tests are presented. Figure 4 shows the results of monotonic drained triaxial shear tests on dense, medium-dense, and loose samples at confining pressures of 50 and 200 kPa. In the dense case, the stress ratio monotonically increases to 1.2 at an axial strain of about 8 % after which a steady state is reached. The global volumetric response is initially contractant followed by dilation just like in real dense sands.

4.2 Influence of confining pressure

Figure 4 also reveals the effects of confining pressure on the mechanical response of the DEM model. The much steeper initial slopes of the curves indicate the much higher strength of dense samples, which also reflect strong evidence of strain hardening and softening effects. At large axial strains, the stress ratios converge to constant values for different initial void ratio. For the volumetric strain, dilatant behaviour is obvious in the dense sands while contraction occurs. The influence of confining pressure is not as great as that of initial void ratio on both the stress-strain curve and volumetric strain versus axial strain curves.

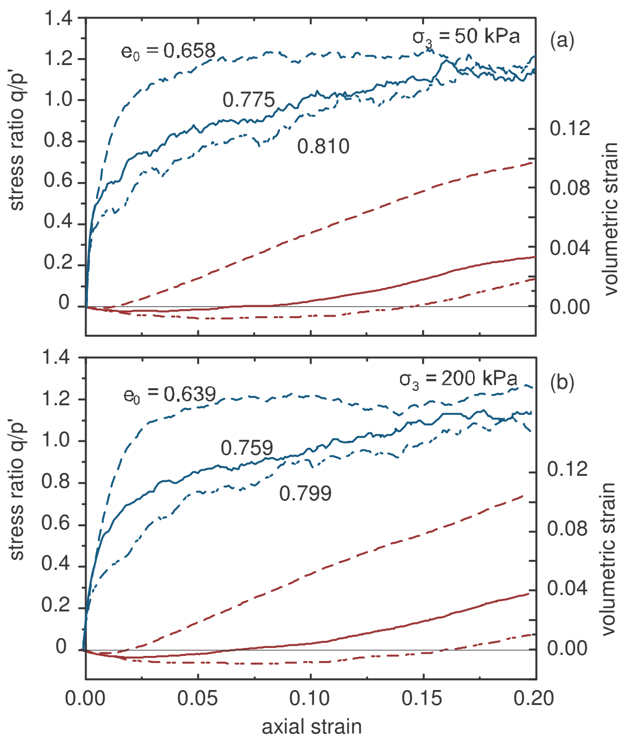

Figure 4. Effects of initial void ratio and confining stress on shear strength and dilatancy characteristics of DEM model under drained conditions

5 MONOTONIC UNDRAINED LOADING

The study of undrained behaviour of soils has important practical applications. For instance, the construction of a building on a clayey soil at a rate faster than the time required for the pore water pressure to dissipate may jeopardize the stability of the building. Other situations correspond to cases when a fast event such as an earthquake loading may induce damage to engineering structures founded on sandy soil. The dramatic increase of pore water pressure may have the effect of reducing the bearing capacity of sandy soil to the extent of leading to tilting and even sinking of superstructures, floating up of buried structures, and permanent lateral displacement of the ground (Kramer, 1996). This last phenomenon is generally known as liquefaction and it is encountered mainly in saturated soil deposits. In the following section, static liquefaction due to monotonic loading is explored, as undrained conditions are considered. Although we talk about undrained conditions, we do not involve water phase in the simulations. The undrained case can be achieved by imposing a no volume change constraint ($d\varepsilon_v = 0$); that is, $d\varepsilon_a = -2d\varepsilon_r$, where $d\varepsilon_a$ and $d\varepsilon_r$ are the axial and radial strains, respectively.

5.1 Influence of initial void ratio

It is generally believed that the initial void ratio is the most important state parameter controlling sand undrained behaviour (Vaid and Sivathayalan, 2000). For instance, sands with low void ratios are susceptible to liquefaction (or limited liquefaction), whereas sands with high void ratios are susceptible to cyclic mobility.

We tried out various initial packing states: loose, medium, and dense (e_0 = 0.686 to 0.743). Figure 5 illustrates the results obtained. In all simulations, the specimen is subjected to an initial effective consolidation pressure of 100 kPa. The stress derived from DEM analysis is in terms of effective stress, as they are fully transmitted through the interparticle contacts. The excess pore pressure is defined by the difference between the initial and current confining stresses $\Delta u = \sigma_{3,i} - \sigma_{3,f}$.

The effect of initial void ratio is clearly demonstrated in the above-mentioned figure since a wide range of undrained responses is obtained. For example, in the case of initial void ratio e_0 = 0.743, the stress-strain curve reaches a peak at small strain (approximately 0.5 %), then due to the collapse of internal fabric and the potential for huge volumetric compaction, a dramatic increase in excess pore pressure along with decrease in shearing resistance takes place with unlimited deformation, if a fluid phase is present. For the medium-dense (e_0 = 0.721) sample, a peak deviatoric stress also appears on the stress-strain curve at small deformations. During this process, the particles arrange themselves and the internal fabric is gradually rebuilt until dilatancy finally dominates the deformation process. Hence, both deviatoric and effective mean stress will increase. For the dense case (e_0 = 0.686), the specimen shows volumetric compaction at very lower shear stress level. As a result, if a fluid was present in the pore space, negative pore pressure will develop after a small accumulation of positive pore pressure as indicated in Figure 5c. The decrease in pore pressure will result in an increase in the effective mean stress, and hence deviatoric stress.

In Figure 5a, the failure line acts as a limiting upper boundary to all the stress paths. The slope of this line is approximately 1.0, which gives a critical state friction angle φ_{cs} = 25.4º. The value is slightly lower than typical critical state friction angles 32º for real sands (Mitchell and Soga, 2005). This is because of the lack of constraints between spherical particles used in our calculations.

Phase transformation, a temporary state of transition from contractive to dilative volumetric responses, is observed for samples with initial void ratios between 0.686 and 0.725 as indicated in Figure 5c. Interestingly, no unique phase transformation curve is found, as displayed in Figure 5a, which is consistent with experimental data (Ishihara, 1993). Quasi-steady state is another interesting phenomenon which is defined as a temporary unstable deformation state at which the soil mass is deforming at constant volume and constant shear stress. However, continued shearing results into an increase of shear stress. This phenomenon is also observed for specimens with initial void ratios of 0.721 and 0.725 (Figure 5b).

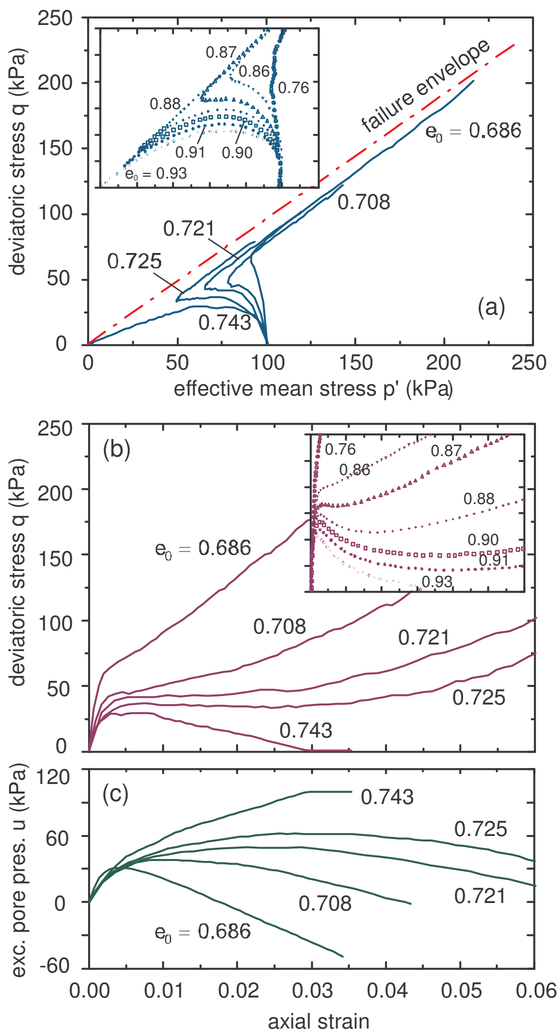

Figure 5. Effects of initial void ratio on shear strength and dilatancy characteristics of DEM model under undrained conditions. The insets show Toyoura sand response (after Verdugo and Ishihara 1996).

For the sake of further comparison, we also have reproduced Verdugo and Ishihara (1996) results in the insets of Figure 5 a,b. These authors have carried out undrained tests on Toyoura sand under various initial void ratios but same initial confining pressure. As one can clearly see, the qualitative pattern of a real sand response was well pictured in our discrete element simulations.

5.2 Influence of confining pressure

The influence of confining stress on the undrained response is shown in Figure 6. A difficulty confronted within our simulation is that we could not achieve a prescribed void ratio in the beginning of setting up the discrete element model. We could only try different initial void ratios in the generation of particles and then apply the isotropic confining pressures 50, 100, and 200 kPa, hoping to arrive close to the targeted void ratio, which is considered as the initial void ratio. In such a process the void ratio varied slightly in each sample, but remained well within the targeted void ratio value. Thus the initial void ratio is slightly different for the three samples shown. However, this slight difference in initial void ratio seems to result into an 'abnormal' behaviour. We call it 'abnormal' because the trend is such that the specimen tends to have flow type failure with the increase of the confining pressure for clean sands. The simulation results show the reverse behaviour and this could be attributed to the variation of the initial void ratio and packing (fabric).

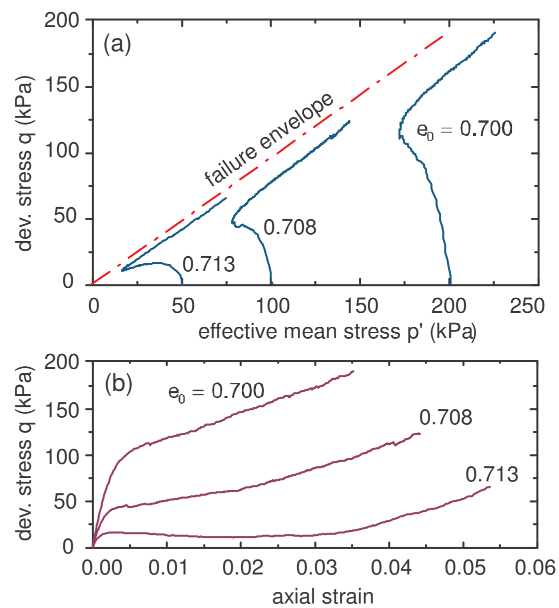

Figure 6. Effects of initial confining stress on shear strength and dilatancy under undrained loading conditions.

6 PROPORTIONAL STRAIN PATHS

In the previous section, it has been demonstrated that undrained condition using the discrete element model played a major role in the liquefaction behaviour of loose sands. In the real practical case, the liquefaction of a sand deposit should not be always assumed to occur in an undrained condition. It would also occur in nonundrained conditions due to pore water pressure redistribution that cause water to drain in and out. Thus, in this section, we investigate the so called proportional strain path tests that mimic such drainage in and out conditions as reported by Chu and Lo (1994) by using discrete element modeling. The reason for studying proportional strain path testing is as follows. The constitutive behaviour of granular material is highly path dependent. Hence, it is essential to study the stability of soils along a wide range of paths. The control of strain path is a better alternative to the control of stress path since in the latter case a sample may run into inadmissible states at the occurrence of instability. The other advantage is that the strain path control generalizes the real drainage condition of soil in the field.

As proposed by Chu et al. (1993), imposed volume changes can be applied to the specimen by the dilatancy ratio $v = d\varepsilon_v/d\gamma$, where $d\varepsilon_v$ and $d\gamma$ are the volumetric and shear strain increments. For axisymmetric conditions in which $d\varepsilon_v = d\varepsilon_a + 2d\varepsilon_r$ and $d\gamma = d\varepsilon_a - d\varepsilon_r$, we obtain $v = (d\varepsilon_a/d\varepsilon_r + 2)/(d\varepsilon_a/d\varepsilon_r - 2)$. From this equation, it is apparent that a particular value of v is related to a proportional strain path in which the specimen deforms at a constant ratio $d\varepsilon_a/d\varepsilon_r$ during shear process. Undrained condition is actually a special case when $v = 0$, while negative and positive values of v refer to forced dilation and compression on the specimen, respectively. Thus, the material response for a wide range of forced dilation or compression could be examined by probing along several proportional strain paths.

In the following, we have selected a dense sample (initial void ratio $e_0 = 0.686$) to numerically carry out the triaxial test along the above described proportional strain paths. Figure 7 shows the results obtained along a variety of proportional strain paths ($v = -0.80$ to 1.08) spanning from large dilation to large compaction, and with an initial confining pressure of 100 kPa. It is noticed that all results display an asymptotic behaviour as shown in Figure 7a. Such an asymptotic behaviour of sand for these paths has been experimentally observed by Chu et al. (1993) using real sand and Al-Mamun (2004) using photoelastic rods (see Figure 7c), and numerically captured by Wan and Guo (2004) using a continuum model. In these works, a phenomenon called 'snap back', in which the stress path changes direction and turns back toward the origin along an asymptotic line after the deviatoric stress increases up to a maximum value, was captured by both experimental and numerical modeling. However, such a 'snap back' phenomenon could not be captured in discrete element simulations.

Let us turn our attention to the case where $v = -0.12$ which corresponds to an overall volume expansion of the specimen. At the beginning of the test, the stress dilatancy is compressive as the mobilized friction angle is small. In order to have an overall expansion, the effective mean stress must decrease (path AB). However, with increasing deformation, friction angle is gradually mobilized resulting into an increase in dilatancy that can exceed the imposed volume expansion rate ($v = -0.12$). In order to satisfy the constraint, the effective mean stress has to increase, see path BC. It is interesting to note that with increasing of v, the response of the assembly changes from hardening behaviour (stable) to strain softening behaviour (unstable). The practical implication of this change is that it is not always sufficient to examine liquefaction issues under undrained condition ($v = 0$) for loose sand. Under some circumstance ($v < 0$), a dense sand that would not liquefy under undrained conditions may display some type of flow failure similar to the liquefaction of loose sands. In-situ conditions may be such that water content redistribution causes water to move into or out of soils layer so as to induce forced volume expansion ($v < 0$) or compaction ($v > 0$), hence based on Figure 7, completely different material behaviours can be obtained.

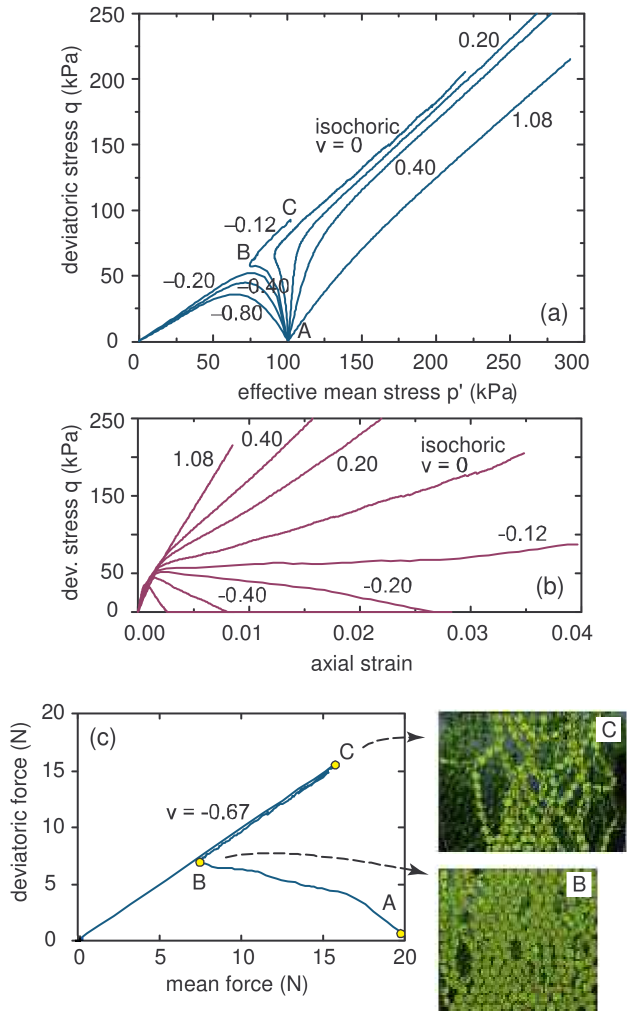

Figure 7. Proportional strain tests in dense assembly using DEM. Proportional strain test using photoelastic rods (after Al-Mamun, 2004)

7 EVOLUTION OF LOCAL VARIABLES

In addition to the macroscopic behaviour depicted in the previous sections, it is also of interest to conduct numerical experiments to examine various local variables (such as the coordination number and fabric tensor) and how they evolve during the shearing process.

7.1 Coordination number

The coordinate number (CN) is used to represent the geometrical feature of contacts for granular media. It is defined as the average number of contacts per particle. Makse et al. (2000) conducted 3D numerical simulations and carbon paper experiments to study random packing of compressible spherical grains under external confining stress. He concluded that the average CN is a function of porosity for friction and frictionless balls. Turning to the topic of particle crushing, the coordination number also plays a very important role since a particle having a higher CN does not easily break due to the better distribution of stress and the confinement produced by its neighbours (Feda, 2002).

A mechanical coordinate number used by Thornton (2000) is herein adapted to calculate CN for dense and loose sample. The average coordinate number is usually defined as CN = N_c/N_p, where N_c is the total number of contacts and N_p is the number of particles. As pointed out by this author, there may be some particles with no contacts or with only one contact at any time of the shear process. These particles are not contributing to the stress of the assembly. Therefore, Thornton (2000) defined a mechanical coordination number CN = $(N_c - N_1)/(N_p - N_0 - N_1)$, where N_0 and N_1 are the number of particle whose CN refers to 0 and 1, respectively. We also eliminate the boundary effect by excluding those balls contacted with walls.

Figure 8 shows the average coordination number versus axial strain in drained tests on both dense and loose samples at a confining pressure of 100 kPa. It is seen that the initial coordination number for the loose sample is around 4.6, which is slightly lower than that of dense sample, i.e. 4.68. For the loose case, the specimen is compressed in the shear process, and therefore more contacts between particles will be formed during the compression process, as indicated in that figure. For the dense sample, the coordination number increases from a value 4.68 to 4.88 after 1 % of axial strain due to the compression of the specimen. After that, the dense sample starts to dilate, which shows a rapid reduction in the coordination number. At large deformations, the CN reaches a steady state value of 4.66 for both dense and loose specimen. This saturation value for CN indicates that there is a rapid reorientation of particles in the dense sample compared to the loose one. At steady state conditions both loose and dense assemblies hold the same number of neighbouring contacts per particle. Therefore, the fabric configurations for dense and loose specimens are sensibly the same at steady state. This will be confirmed further in the next section while discussing the fabric tensor.

Similar results are obtained after the particle rotation is prohibited for both dense and loose sample as also shown in Figure 8. Due to particle rotation restraint, even the loose sample shows tendency to dilate Thus the CN for the loose sample shows a similar pattern as for the dense sample, i.e., CN first increases due to compression and then decreases due to dilation. Another difference from those results with particle rotation is that the CN's for both dense and loose sample do not converge to a constant value due to the increase of confining pressure in the latter part of deformation.

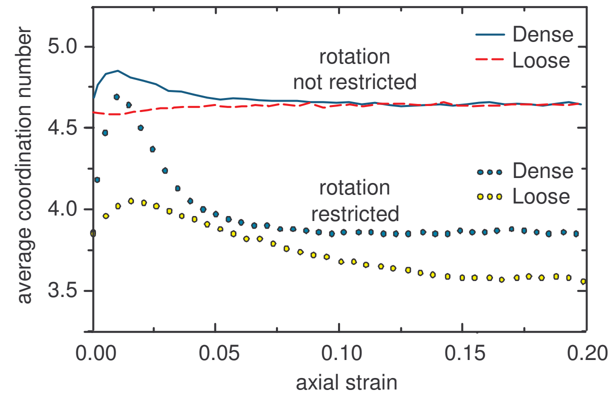

Figure 8. Average coordination number in drained tests on both dense and loose samples with rotation not restricted and rotation restricted cases

7.2 Fabric and anisotropy

Granular materials, such as sands, consist of non-spherical particles with random packing, but statistical arrangements. The nomenclature 'fabric' has been used to represent the spatial arrangement of particles and voids. Anisotropy is another fundamental concept. According to Oda (1993), there are two sources for anisotropy, namely anisotropy by preferred orientation of non-spherical particles and anisotropy by concentration of contact normals. Here we only consider the later one because we use spherical particles in this research. A fabric tensor is employed to analyze the anisotropic microstructure of the material in this section.

Mataska's fabric tensor is implemented here due to its simplicity (Thornton, 2000):

$$\theta_{ij} = \frac{1}{N_c}\sum_{i,j=1}^{N_c} n_i n_j \qquad [1]$$

where n is the component of the direction of contact normal.

In Figure 9, we plot our results in terms of deviatoric fabric $(\theta_1 - \theta_3)$, a concept similar to that of deviatoric stress $(\sigma_1 - \sigma_3)$. This figure shows the deviatoric fabric versus axial strain for both dense and loose samples. It is found that the induced anisotropy increases to a maximum value which is dependent on the initial void ratio. It is interesting to note that the deviatoric fabric curve has a similar shape to the stress-strain curve. As we mentioned in the previous section, the fabric configuration for dense and loose specimens is the same at steady state. At large deformations (20 % of axial strain), the principal component of the fabric tensor are θ_1 = 0.403, θ_2 = 0.299, and θ_3 = 0.297 for the dense sample, and θ_1 = 0.396, θ_2 = 0.303, and θ_3 = 0.300 for the loose sample. These values are more or less the same in both cases. Figure 9 also gives the evolution of the deviatoric fabric with particle rotation restriction. The fabric configurations for dense and loose specimens also seem to be the same at the steady state under this rotation restriction.

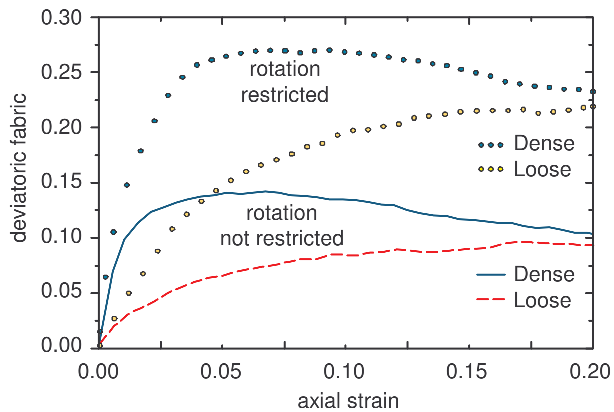

Figure 9. Average coordination number in drained tests on both dense and loose samples with rotation not restricted and rotation restricted cases

8 CONCLUSIONS

The results presented in this paper clearly show the power of the discrete element technique to simulate granular soil behaviour under generalized loading paths. A number of features observed in the laboratory are well reproduced by numerical simulations. They include: (1) the shape of stress-strain curve, dilative volumetric behaviour for dense sample and pressure dependency of shear strength found in drained conditions; (2) liquefaction due to the build-up of the excess pore pressure, phase transformation points and quasi-steady state exhibited in undrained conditions; and (3) liquefaction of dense material under proportional strain paths. Numerical simulations highlight the effect of inter-particle friction on the triaxial compression behaviour of granular materials, which can result into higher strength and dilation rate with the increase of the interparticle friction under drained condition. The numerical response shows that there is considerable rotation when using spherical particles, which results in lower peak and steady state friction angles. The analysis of the various internal variables indicated that average coordination numbers are the same at the steady state for both dense and loose samples under the drained condition at the same confining pressure. On the other hand, the anisotropy of the granular system interpreted in terms of deviatoric fabric reaches a steady state for both dense and loose samples under both free and restricted particle rotations.

From the above simulations, we can see that DEM is quite an efficient and robust tool to study the loading response and the constitutive behaviour of granular materials. Their generality and potential to unify all types of loading has already been mentioned.

ACKNOWLEDGEMENTS

The financial support provided by the Natural Science and Engineering Research Council (NSERC) is acknowledged.

REFERENCES

Al-Mamun, M.A.M. 2004. *Experimental Study of Granular Material Behavior and Microstructure in a Photoelastic Disk Assembly*. MSc Thesis, U of Calgary, Canada.

Bardet, J.P. 1994. Numerical Simulations of the Incremen-tal Responses of Idealized Granular Materials, *Intl J. of Plasticity* 10: 879-908.

Chang, C.S., Chang, Y. Kabir, M. 1992. Micromechanics Modelling for the Stress-Strain Behavior of Granular Soil - I: Theory. *J. Geot. Eng.* 118(12): 1959-1974.

Chu, J. and Lo, S.C.R. 1994. Asymptotic Behaviour of a Granular Soil in Strain Path Testing. *Géotechnique* 44(1): 65-82.

Chu, J., Lo, S.C.R. and Lee, I.K. 1993. Instability of Granular Soils under Strain Path Testing. *J. Geotechnical Eng.* 119(5): 874-892.

Cundall, P.A. 1971. A Computer Model for Simulating Progressive Large-Scale Movements in Blocky Rock Mechanics. In: *Proc. Symposium Intl Soc. Rock Mech.* Nancy, France, 2: 129-136.

Cundall, P.A. and Strack, O.D.L. 1979. A Discrete Num. Model for Granular Assemblies. *Géotechnique* 29(1): 47-65.

Feda, J. 2002. Notes on the Effect of Grain Crushing on the Granular Soil Behaviour. *Engineering Geology J.*, 63(1-2): 93-98.

Guo, P. 2000. *Modelling Granular Materials with respect to Stress-Dilatancy and Fabric: a Fundamental Approach.* PhD Thesis, U of Calgary, Canada.

Ishihara, K. 1993. Liquefaction and Flow Failure during Earthquakes. *Géotechnique* 43(3): 351-415

Itasca. 1999. *PFC 3D - User Manual*. Itasca Consulting Group, Minneapolis.

Kramer, S.L. 1996. *Geotechnical Earthquake Engineering*. Prentice-Hall, Englewood Cliffs, NJ, USA.

Makse, H.A., Johnson, D.L. and Schwartz, L.M. 2000. Packing of Compressible Granular Materials. *Physical Review Letters*, 84(18): 4160-4163.

Mitchell, J.K. and Soga, K. 2005. *Fundamentals of Soil Behavior*. Wiley, New Jersey, USA.

Oda, M. 1993. Inherent and Induced Anisotropy in Plasticity Theory of Granular Soils. *Mechanics of Materials J.* 16(1-2): 35-45.

Oda, M., Konishi J. and Nemat-Nasser, S. 1982. Experimental Micromechanical Evaluation of Strength of Granular Materials: Effect of Particle Rolling. *Mechanics of Materials J.* 1: 267-283.

Thornton, C. 2000. Numerical Simulations of Deviatoric Shear Deformation of Granular Media. *Géotechnique* 50(1): 43-54.

Vaid, Y.P. and Sivathayalan, S. 2000. Fundamental Factors Affecting Liquefaction Susceptibility of Sands. *Canadian Geotechnical Journal* 37: 592-606.

Verdugo, R. and Ishihara, K. 1996. The Steady State of Sandy Soils. *Soils and Foundations*, 36(2): 81-91.

Wan, R.G. and Guo, P. 2004. Stress-Dilatancy and Fabric Dependencies on Sand Behavior. *J. Eng. Mechanics.* 130(6): 635-645.